Electrostatic Force Study with Floating Wave Function. Comparative Study on the Origins of the Molecular Shapes of CH_3^+ and NH_3

Hiroshi NAKATSUJI, Kazuo MATSUDA, and Teijiro YONEZAWA

Department of Hydrocarbon Chemistry, Faculty of Engineering, Kyoto University, Kyoto 606

(Received October 7, 1977)

The force and density origins of the molecular shapes of CH_3^+ and NH_3 are studied comparatively on the basis of the floating wave functions which satisfy the Hellmann-Feynman theorem for the forces acting on the terminal protons. It is confirmed quantitatively that the previous concepts of the electrostatic force (ESF) theory correctly grasp the origins of the molecular shapes. Namely, the *density-guiding rule* which states that the nuclei are pulled in the direction of the electron-cloud reorganization (*i.e.*, the electron-cloud preceding and incomplete following), is verified as the density origin. The force origin which is the AD and EC forces reflects and quantifies the density origin. The roles of the other forces are also easily predicted by the ESF theory.

It is now well established that the force concept based on the Hellmann-Feynman (H-F) theorem[1] gives a quite intuitive basis for the understandings of various chemical phenomena.[2–13] Though such approaches had been thought to have a difficulty in the reliability of the *calculated* H-F force,[14] it is well known that if we use the floating wave function[15–17] the H-F theorem is satisfied, so that the intuitive force concept gains also a sufficient reliability, which is the same as in the conventional energetics.[18] In this series of papers,[19] we investigate quantitatively the force and density origins of some molecular geometries and chemical reactions on the basis of the floating wave functions. A purpose of this series is to give a sufficient quantitative basis for the force theoretic approach. This is an urgent necessary step in comparison with the conventional energetics, and moreover such studies will give a basis to investigate more complex phenomena than those studied so far by this approach. Another purpose of this series (especially in the first few ones) lies in the verification of the concepts of the electrostatic force (ESF) theory[8–11] from a purely theoretical *ab initio* point of view. Though the success of the ESF theory, especially in the field of molecular geometry[8] (*i. e.*, the theory has predicted the geometries of various molecules *without* calculations in agreement with *experiments*), is itself a strong proof for the validity of the ESF concepts, we aim in these studies a more direct verification.

Due to the H-F theorem[1] the force acting on a nucleus is determined solely by the electron density $\rho(\boldsymbol{r})$ (the nuclear part is trivial). It is one of the basic observables in quantum mechanics, and due to Hohenberg and Kohn's theorem,[20] it includes all of the informations of the system. Therefore, we can express the origins of various molecular processes with either the force or the density behaviors along the processes.[21] The density origin is the reorganization of the electron density along the process,[7,9] which is characterized generally as the electron-cloud preceding or the electron cloud incomplete following which works respectively to accelerate or resist the process.[9] In other words, *the nuclei are pulled in the direction of the electron-cloud reorganization.* This simple rule constitutes a guiding principle for nuclear rearrangement processes on the basis of the behaviors of the electron density alone,[8b,9] and may be called a *density guide* or *density-guiding rule.* The force origin reflects and quantifies this origin. The partitioning of the H-F force into the atomic dipole (AD), exchange (EC), and extended gross charge (EGC) forces[8] gives a way to study quantitatively the regional role of the electron density. They are parallel with the chemical concepts like lone pair, bond, and gross charge, respectively.[8] The AD and EC forces are of particular importance since the electron-cloud preceding and incomplete following manifest themselves mainly in the AD and EC forces.[9] This is a reason[9] why these forces have played such important roles in the ESF theory applied to molecular geometries,[8b,9] chemical reactions, [10]and long-range forces.[11]

When the ESF concepts are applied to the AH_3 molecules, the origins of their shapes are expected as follows.[8,9] Namely, when the molecule is bent slightly from the planar form, the electron density in the atomic (A and H) and overlap (A–H) regions will precede (in the pyramidal molecules) or incompletely follow (in the planar molecules) the nuclear bending displacement. The constituent nuclei will therefore be pulled by the AD and EC forces in the bending or planarizing direction, respectively, and will move in the direction to the equilibrium geometry. Though we tried to verify this picture in the previous paper,[9b] it was insufficient since the wave function used there did not satisfy the H-F theorem. Here, we want to examine this picture quantitatively on the basis of the floating wavefunctions.

In the previous communication of this series,[19] we have reported a simpler way of obtaining the floating wave function. Namely, if we limit ourselves to the force $\boldsymbol{F}_A$ acting on a special nucleus A of the system, it is sufficient that only the AO's belonging to the atom A be floated and their centers be determined variationally. The resultant wave function gives a reliable H-F force $\boldsymbol{F}_A$ which satisfies the H-F theorem. Based on this fact, we have studied quantitatively the force and density origins of the molecular shape of H_2O, limiting ourselves to the transverse force acting on the terminal protons. It has been confirmed that the ESF picture as described in the preceding paragraph correctly grasps the origin of the bent geometry of H_2O.[19] In this paper, we will examine further such ESF concept of the origins of the molecular shapes of CH_3^+ and NH_3. We will again limit ourselves to the transverse force acting on the terminal protons and investigate

the behaviors of the electron density in the A–H region during the out-of-plane bending process. It will give a comparative basis for the origins of the molecular shapes of planar and pyramidal molecules.

We note that in the previous extensive applications of the ESF theory to various molecular geometries,[8] we have mostly concerned with the force acting on the central nucleus (*e.g.* the nucleus A in the AH_3 molecule). It is clear from these studies that such method is easier and more fruitful for constructing a predictive theory of molecular geometries without calculations.[8] However, for the AH_3 molecules, the calculations of the floating wave functions become more elaborate for the force $\boldsymbol{F}_A$ than for the force $\boldsymbol{F}_H$, since the numbers of the basis AO's are smaller for H than for the heavier atom A. Therefore, we will postpone the *ab initio* study of $\boldsymbol{F}_A$ in the subsequent paper. We remark however that for general molecules (*e.g.* AX_n molecules) the floating wave function is more easily obtained for $\boldsymbol{F}_A$ than for $\boldsymbol{F}_X$, in contrast to the AH_3 molecules.

Floating Wave Functions for CH_3^+ and NH_3

The SCF-MO calculations have been carried out with the use of the minimal STO-3G bases[22] with the standard exponents reported by Hehre *et al.*[23] We have used the modified version of the Gaussian 70 Program. In obtaining the floating wave function, we have adopted a simpler procedure noted previously.[19] Namely, we have floated only the ls AO's on the terminal protons and the other AO's on carbon and nitrogen, which are the 1s, 2s, $2p_x$, $2p_y$, and $2p_z$ AO's were kept fixed on the nuclei. Therefore, the present wave functions satisfy the H-F theorem for the forces acting on the terminal protons. The C–H and N–H lengths of CH_3^+ and NH_3 were kept fixed at, respectively, 1.120 and 1.033 Å which are the lengths optimized by the STO-3G calculations.[24] The experimental N–H length is 1.012 Å.[24] We have calculated the transverse force acting on the terminal protons and also the behaviors of the electron density in the A–H region at various out-of-plane bending angles θ. Several quantities pertinent to the present analysis are defined in Fig. 1.

Tables 1 and 2 give the variationally best positions of the $1s_H$ floating AO's (FAO's) of CH_3^+ and NH_3, respectively, and the effects of floating on the SCF energy and the H-F transverse force $\boldsymbol{F}_{H\perp}$ acting on the terminal protons. The H-F force is partitioned

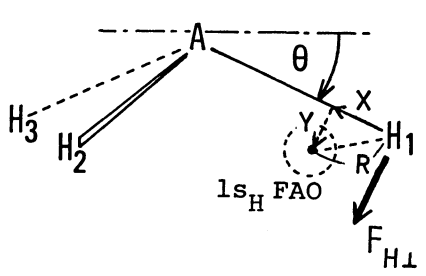

Fig. 1. Definitions of the out-of-plane bending coordinate θ, the centers of the $1s_H$ FAO's and the transverse force acting on the terminal protons $\boldsymbol{F}_{H\perp}$ for the AH_3 molecules.

into the atomic dipole (AD), exchange (EC), and extended gross charge (EGC) forces with a slight modification of the previous ones used for the non-floating wave function.[8,25] The values in parentheses are those obtained from the non-floating wave functions. The distance R of the FAO center from the proton is about 0.04 Å for CH_3^+ and about 0.02 Å for NH_3. It was about 0.03 Å for H_2O.[19] They are all in the same order of magnitude as those reported previously for H_2 by Shull and Ebbing.[26] Though the FAO center of CH_3^+ lies outside of the pyramid ($Y<0$), that of NH_3 lies inside of the pyramid ($Y>0$). For both cases, the distance Y is sensitive to the bending angle θ, though the distance X is insensitive. (The latter would be sensitive to the stretching mode). As will be seen later, these behaviors of the FAO's are closely related with the manners of the electron-cloud reorganization during the out-of-plane bending processes. The floating of the AO's gives a freedom in the wave function to describe such behaviors of the electron density especially in the atomic regions.

The floating of the $1s_H$ AO's was not effective to improve the SCF energy, as studied earier by Shull and Ebbing for the hydrogen molecule.[26] The energy lowering obtained by the floating is about 0.008 a.u. (5 kcal/mol) for CH_3^+ and 0.003 a.u. (2 kcal/mol) for NH_3. They are very small in comparison with those obtained by the other ways of improving the wave function. For example, the addition of the polarization function on hydrogen, which also describes the polarization of the electron density in the atomic region, lowers the SCF energy of NH_3 by 0.058 a.u. in the similar calculations of the STO-3G level[10b] and by 0.039 a.u. in the calculations of double-zeta accuracy.[27] However, in contrast to the floating method, it is generally difficult in such procedures to assure the complete satisfaction of the H-F theorem, so long as the basis set is incomplete.

Though the effect of floating is quite small for the SCF energy, it is very large and important for the H-F force. As seen from Tables 1 and 2, the errors for the H-F theorem are essentially zero in the floating wave functions, though they are large in the non-floating wave functions especially for NH_3. The small non-zero errors still remaining in the floating wave functions of CH_3^+ are the numerical errors in determining the optimal FAO centers. These error values have been obtained by calculating directly the error term for the H-F theorem, *i.e.*, the term $\langle \partial\Psi/\partial \boldsymbol{R}_A | H | \Psi\rangle + \langle \Psi | H | \partial\Psi/\partial \boldsymbol{R}_A\rangle$, by the method developed by Moccia *et al.*[28] Thus, it is confirmed that the present floating wave function satisfies the H-F theorem for the force acting on the terminal protons.

As seen from Table 1, the equilibrium shape of CH_3^+ is calculated to be planar from both the floating and non-floating wave functions. The planar geometry of CH_3^+ is well established by the previous studies.[24,29] The out-of-plane bending force constant calculated from the H-F force is 0.93 md/Å with the floating wave function and 0.82 md/Å with the non-floating wave function. The former should of course be identical with the result obtained from the SCF energy

Table 1. Center of $1s_H$ FAO and the effects of floating on the SCF energy E and the H-F force $F_{H\perp}$ for CH_3^+

θ (Deg)	FAO Center (Å)			$-\Delta E \times 10^3$ (au)	$F_{H\perp} \times 10^2$ (au)[a]					
	X	Y	R		Total H-F	Error	AD	EC(H-C)	EC(H--H)[b]	EGC
0 (Eq)	0.041	0.0	0.041	8.1	0.0 (0.0)	0.0 (0.0)	0.0 (0.0)	0.0 (0.0)	0.0 (0.0)	0.0 (0.0)
5	0.041	−0.0006	0.041	8.1	−1.10(−0.97)	−0.07(−0.19)	−0.08(0.0)	−0.69(−0.70)	−0.08(−0.07)	−0.24(−0.21)
10	0.041	−0.0018	0.041	8.0	−2.34(−1.95)	0.00(−0.38)	−0.27(0.0)	−1.35(−1.40)	−0.17(−0.14)	−0.55(−0.41)
15	0.040	−0.0033	0.040	7.9	−3.60(−2.96)	0.05(−0.57)	−0.44(0.0)	−2.04(−2.12)	−0.28(−0.23)	−0.85(−0.62)
24.3	0.039	−0.0042	0.039	7.6	−5.93(−5.02)	−0.07(−1.09)	−0.63(0.0)	−3.42(−3.52)	−0.55(−0.47)	−1.32(−1.03)

a) The values in parentheses are obtained from the non-floating wave functions. b) This value is the sum of the two identical EC(H--H) forces.

Table 2. Center of $1s_H$ FAO and the effects of floating on the SCF energy E and the H-F force $F_{H\perp}$ for NH_3

θ (Deg)	FAO Center (Å)			$-\Delta E \times 10^3$ (au)	$F_{H\perp} \times 10^2$ (au)[a]					
	X	Y	R		Total H-F	Error	AD	EC(H-N)	EC(H--H)[b]	EGC
0	0.019	0.0	0.019	2.3	0.0 (0.0)	0.0 (0.0)	0.0 (0.0)	0.0 (0.0)	0.0 (0.0)	0.0 (0.0)
10	0.020	0.009	0.022	2.9	1.24(−0.96)	0.00(2.11)	1.60(0.0)	0.68(0.93)	−0.17(−0.29)	−0.87(−1.60)
15	0.020	0.012	0.023	3.3	1.30(−1.55)	0.00(2.79)	2.08(0.0)	0.71(1.05)	−0.29(−0.45)	−1.20(−2.15)
24.3(Eq)	0.020	0.012	0.023	3.6	0.00(−3.12)	0.00(3.12)	2.29(0.0)	−0.07(0.31)	−0.62(−0.80)	−1.59(−2.63)
40	0.021	0.008	0.022	3.6	−6.35(−8.55)	0.00(2.09)	1.63(0.0)	−3.66(−3.36)	−1.68(−1.79)	−2.64(−3.40)

a) The values in parentheses are obtained from the non-floating wave functions. b) This value is the sum of the two identical EC(H--H) forces.

curve. On the other hand, for NH_3 (Table 2), the effect of the floating on the H-F force is essential even for the qualitative calculation of the equilibrium shape. With the non-floating wave function, the shape is calculated to be planar! This is because the minimal STO-3G basis fixed on the nuclei is far from complete and can not describe the polarization of the electron density in the atomic region near the proton (see below). However, with the floating wave function, NH_3 is calculated to be pyramidal with $\theta_{eq}=24.3°$ ($\angle HNH=104.2°$) which is just the same as the STO-3G geometry.[24] The experimental value is $\theta_{eq}=22.1°$ ($\angle HNH=106.7°$).[24]

The partitioning of the H-F force into the AD, EC, and EGC forces clarifies the details how the floating of the $1s_H$ AO's improves the H-F force. As seen in Tables 1 and 2, the largest effect of the floating occurs for the AD force. It improves most of the errors included in the non-fioating H-F force (50—80% for CH_3^+ and 70—80% for NH_3). This is because the H-F force is most sensitive to the errors in the region near the nucleus. In the non-floating wave function, the AD force was always zero since the present basis AO's do not include the polarization functions on the hydrogen atom. In the floating wave function, it arises because the $1s_H$ AO density floating apart from the proton pulls it in the direction of the floating. For CH_3^+, Y is negative so that the induced AD force is negative, while for NH_3, Y is positive so that the AD force is positive. In both cases, the distance Y and the AD force are parallel. The second largest effect of the floating occurs for the EGC force. For CH_3^+ the floating enlarges the repulsive EGC force, whereas for NH_3 it diminishes: in CH_3^+ the outward floating ($Y<0$) of the $1s_H$ AO makes its proton more bare so that the repulsion increases, while in NH_3 the AO floated inward of the proton ($Y>0$) shields it more effectively from the repulsion with the other protons. These "self-shielding" effects have arisen from the modification of the partitioning as given in Ref. 25. The effect of floating is smallest for the EC force as expected from the small distance Y in comparison with the bond distance. The effect is smaller for CH_3^+ than for NH_3 since Y is smaller for CH_3^+.

Origin of the Molecular Shape

In this section we study quantitatively the force and density origins of the molecular shapes of CH_3^+ and NH_3. We investigate the behaviors of the electron density and the induced forces acting on the terminal protons during the out-of-plane bending process. Since the present floating wave function satisfies the H-F theorem, we can examine quantitatively the concepts developed previously in the ESF theory.

First, we study the density and force origins of the planar geometry of CH_3^+. Figure 2 shows the change in the electron density of CH_3^+ when it is bent by 15° from the planar form. The density at $\theta=0°$, which is symmetric with respect to the CH_3 plane, was subtracted from that at $\theta=15°$ with superposing the C–H_1 axis on the right hand side.[30] This figure is then meaningful only in the region near the C–H_1 axis. The real and dotted lines show respectively the increase and decrease in the electron density. From this figure, we see that the reorganization of the C–H bond density of CH_3^+ shows a typical feature of the electron-cloud incomplete following in the out-of-plane bending process. Namely, as seen from the increase and the decrease in the regions above and below the C–H_1 axis, respectively, the C–H bond density at $\theta=15°$ does not lie on the C–H axis, but follows with lag the out-of-plane bending displacement of the C–H axis. The bond density, following back of the C–H axis, will pull the terminal proton in the reverse direction to θ, so that the molecule will be restored again to the planar form: i.e., the equilibrium geometry of CH_3^+ is expected to be planar in accordance with the previous studies.[29] This is the result of the density-guiding rule applied to the geometry of CH_3^+.

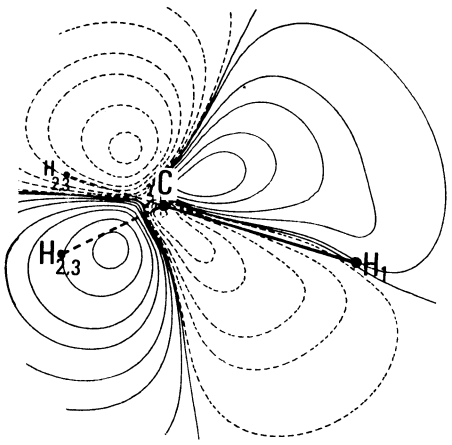

Fig. 2. Electron-cloud reorganization in CH_3^+ at $\theta=15°$ in the C–H_1 region. The density at $\theta=0°$ was subtracted from that at $\theta=15°$ with superposing the C–H_1 axes. The contours are at 0.0, ±0.001, ±0.005, ±0.01, +0.015, −0.02, +0.025, ±0.04, ±0.07, ±0.1, and ±0.15 au (real lines ≥0, dashed lines <0).

The above density origin is verified from Fig. 3 which shows the analysis of the transverse force $\boldsymbol{F}_{H\perp}$ acting in CH_3^+ during the bending process. The dotted line shows the SCF energy curve. Throughout the bending process, the protons of CH_3^+ receive the planarizing forces; *i.e.*, the molecule is calculated to be planar. In CH_3^+ all of the force components are cooperative to make the molecule planar. Among these, the dominant force origin is the EC(H–C) force. It arises from the incomplete following of the C–H bond density as depicted in Fig. 2. [If the C–H bond density always lies on the C–H axis (complete following), it does not induce the *transverse* EC(H–C) force.] The electron-cloud incomplete following in the atomic region manifests itself in the AD force. It has arisen through the floating of the $1s_H$ AO's. The behaviors of the $1s_H$ FAO's seen from the distance Y given in Table 1 clearly show the occurrence of the electron-cloud incomplete following in the atomic region. The sum of the EC (H–C) force and the AD force accounts most (≈70%) of the total planarizing force.

Thus, we conclude that the density origin of the

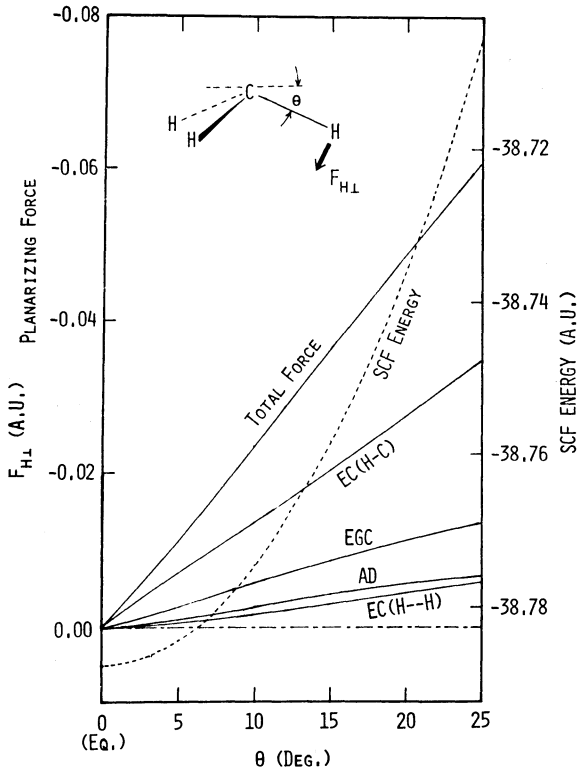

Fig. 3. The transverse force $\boldsymbol{F}_{H\perp}$ and the SCF energy *vs.* the out-of-plane bending angle θ for CH_3^+.

planar shape of CH_3^+ lies in the occurrence of the electron-cloud incomplete following of the C–H bond density during the out-of-plane bending process. We have confirmed that the electron-cloud incomplete following as depicted in Fig. 2 occurs over the all angular range studied here ($0°<\theta<24.3°$) and that the extent increases with the increase in the bending angle θ. The force origin, which is the EC(H–C) and AD forces (mostly the EC(H–C) force), reflects and confirms this density origin.

In Fig. 3, the other minor force components, *i.e.*, the EGC and EC(H--H) forces are also cooperative to make CH_3^+ planar. We note that the roles of these forces are also naturally understood. Namely, in CH_3^+, the net gross charges of the terminal hydrogens are positive, so that the EGC force which represents the interaction between the shielded protons would be repulsive. The EC(H--H) force would also be repulsive since it arises from the exchange interaction between the doubly occupied C–H bond orbitals. Among these, the origin of the EC(H--H) force may be included in the electron-cloud incomplete following as has been discussed previously for the similar interaction during the internal rotation of ethane.[8]

We next investigate the density and force origins of the pyramidal shape of NH_3. In Fig. 4 we have depicted the electron-cloud reorganizations in NH_3 at the bending angles $\theta=15$, 24.3 (calculated equilibrium), and 40°. They are defined similarly to Fig. 2.[30,31] As seen from Fig. 4, the electron-cloud reorganization in NH_3 is quite different from that in CH_3^+. At $\theta=15°$ (Fig. 4(A)), the behavior of the N–H bond density of NH_3 shows a typical feature of the electron-

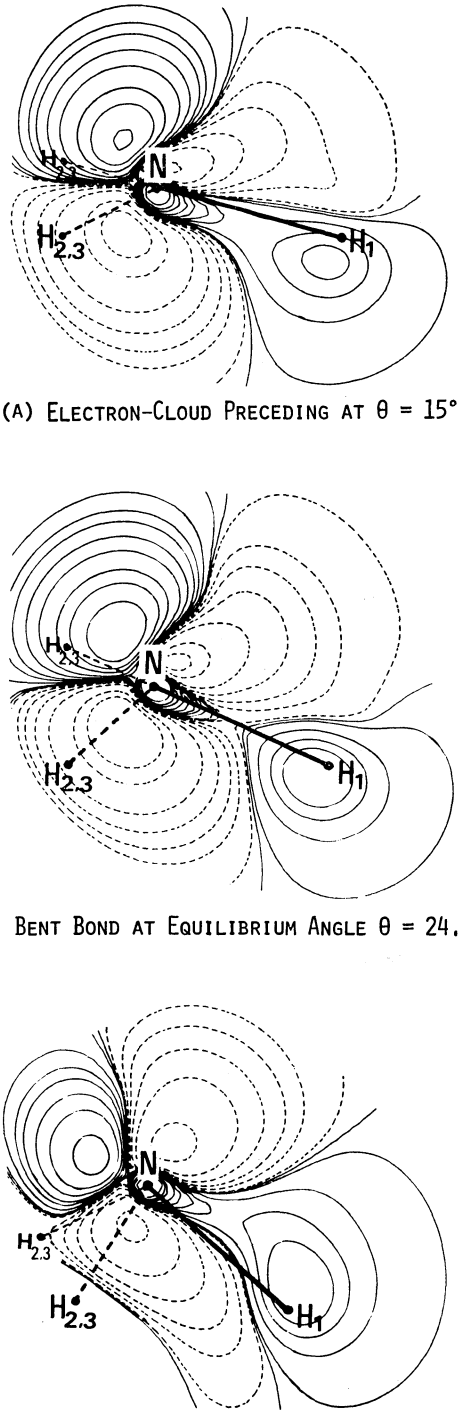

Fig. 4. Electron-cloud reorganization in NH_3 in the N-H_1 region during the out-of-plane bending process. (A) $\Delta\rho(15°)=\rho(15°)-\rho(0°)$, (B) $\Delta\rho(24.3°)=\rho(24.3°)-\rho(0°)$, (C) $\Delta\rho(40°)=\rho(40°)-\rho(24.3°)$. In subtracting the reference density, the N-H_1 axes were superposed. The levels of the contours are the same as those given in Fig. 2.

cloud preceding.[9] Namely, the increase and the decrease in the electron density in the regions below and above the N-H_1 axis, respectively, shows that the N–H bond density does not lie on the N–H axis, but

bends more than the N–H axis. The N–H density, preceding ahead of the bending movement of the N–H axis, will pull the terminal proton in the bending direction, so that the bending process will be accelerated further. Therefore, the stable shape of NH_3 is expected to be pyramidal in agreement with the experiment. When the molecule reaches the equilibrium angle ($\theta=24.3°$), such preceding character almost vanishes as seen in Fig. 4(B). The bond electron density becomes almost symmetric with respect to the N–H axis in order to keep the terminal proton in an electrostatic equilibrium with respect to the transverse force. A small preceding character seen especially in the atomic region near H shows an inward bent bond which is necessary to cancel with the interproton repulsions at the equilibrium geometry.[9b] When the molecule is bent further from the equilibrium angle, the N–H bond density again dispart from the N–H axis, and the electron-cloud incomplete following occurs as seen in Fig. 4(C). This behavior is just reverse to that seen at $\theta=15°$ (Fig. 4(A)). The N–H bond density, following back of the N–H axis, will pull the terminal proton upwards so that the molecule will be restored again to the equilibrium angle. In summary, the electron-cloud reorganization in NH_3 during the out-of-plane bending process is characterized by the electron-cloud preceding in the region $0°<\theta<24.3°$ and the electron-cloud incomplete following in the region $\theta>24.3°$. From the density guide, we may expect the equilibrium angle at about 24.3° where the density behavior turns reverse from the preceding to the incomplete following.

In Fig. 5 we have shown the analysis of the transverse force $\boldsymbol{F}_{H\perp}$ in NH_3 during the out-of-plane bending process. By virtue of the floating, the equilibrium angle calculated from the H-F force agrees with that obtained from the SCF energy curve. Among the force components shown in Fig. 5, only the AD and EC(H–N) forces work to accelerate the bending process in the range $0°<\theta<\theta_{eq}$. Therefore, the force orgin of the pyramidal shape of NH_3 is the AD and EC(H–N) forces which reflect the electron-cloud preceding in the atomic and overlap regions, respectively. The other forces, *i.e.*, the EGC and EC(H--H) forces, work to resist the bending process by the same reason as explained for CH_3^+. This fact clearly confirms the importance of the electron-cloud preceding in the region $0°<\theta<\theta_{eq}$. Without it, the pyramidal shape of NH_3 can not be realized. At the equilibrium angle (24.3°), the repulsive EGC and EC(H--H) forces are canceled out by the AD force. The EC(H–N) force is almost zero at this angle. This means that the inward bent bond character at the equilibrium geometry, which is necessary to cancel the interproton repulsions, occurs mostly in the atomic region near the proton (see Fig. 4(B)). In the angular region $\theta>\theta_{eq}$, the force on the proton works to restore the molecule again to the equilibrium angle. It arises from the EC(H–N), EGC, and EC(H–H) forces. The AD force contributes to the restoring force by diminishing its bending role. Among these, the slope of the EC(H–N) force is steepest so that it becomes the most important component of the restoring force. It reflects the electron-cloud incomplete following depicted in Fig. 4(C) at $\theta=40°$. Thus, it is confirmed that the density guide applied to the geometry of NH_3 certainly grasps the most important factors of the force components. The dominant force origin, which is the AD and EC(H–N) forces, reflects and confirms the density origin summarized in the preceding paragraph.

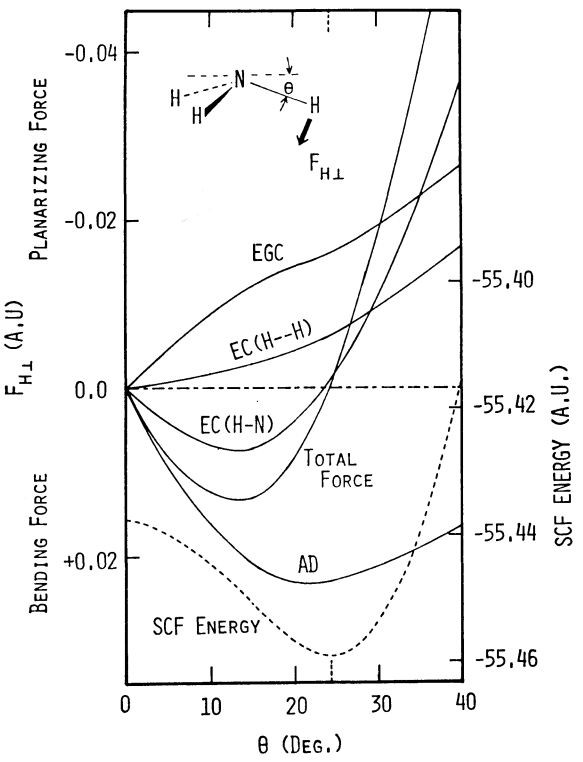

Fig. 5. The transverse force $\boldsymbol{F}_{H\perp}$ and the SCF energy *vs.* the out-of-plane bending angle θ for NH_3.

It is interesting to note that the density and force origins of the pyramidal shape of NH_3 are quite similar to those of the bent geometry of H_2O reported previously.[19] On the basis of the generality of the density-guiding rule as discussed in the previous paper,[9] we believe that this similarlity in the force and density origin is actually a more general one which is correct at least for any kind of AH_2, AH_3, and related substituted molecules having bent or pyramidal geometries. By the same reason, the force and density origins shown here for CH_3^+ would also be common to the above types of molecules having linear or planar geometries.

It would also be worthwhile to remark that for both CH_3^+ and NH_3, the curves for the EC(H–A) forces cross the zero line at about the equilibrium angle; *i.e.*, at $\theta=0°$ for CH_3^+ and at $\theta=23°$ for NH_3. The same is also true for H_2O; *i.e.*, just at $\theta=\theta_{eq}$ (=40°) (see Fig. 3 in Ref. 19). If this is true more generally, we can estimate the equilibrium angle only from the EC(H–A) force, and furthermore, since the effect of the floating is small for the EC(H–A) force, this procedure would be possible *even* with the *non*-floating wave functions. Actually, such procedure with the use of the non-floating wave function gives the equilibrium angle 0° for CH_3^+, 25° for NH_3 (see Tables 1 and 2), and 40° for H_2O. These values agree surprisingly well

with those obtained from the floating wave functions which are 0, 24.3, and 40°, respectively. The experimental values are 0, 22.1, and 37.8°, respectively.[24]

Density Behavior Reflected in the Potential Energy Curve

It is well known that the energy is an explicit function of not only the electron density $\rho(\boldsymbol{r})$ but also the off-diagonal first-order density matrix $\rho(\boldsymbol{r}|\boldsymbol{r}')$ and the second-order density matrix $\Gamma(\boldsymbol{r}_1, \boldsymbol{r}_2)$.[32] The latter two functions are much more complicated than the electron density. On the other hand, the H–F theorem states that the force acting on a nucleus is determined solely by the electron density $\rho(\boldsymbol{r})$ surrounding the nucleus. The nuclear repulsion term is trivial. Therefore, if we integrate the H-F force along the process, we can obtain the potential energy curve solely from the dynamic behavior of the electron density during the nuclear rearrangement process. Though this is trivial, the underlying concept of this procedure is simpler and more visual than that of the conventional energetics. A condition for the (numerical) equivalence between the conventional energetics and the *integrated* H-F force approach is the holdness of the H-F theorem, which the present floating wave function satisfies. Then, we examine here such idea for CH_3^+ and NH_3 by integrating the force curves given in Figs. 3 and 5.

Figures 6 and 7 show the enrgy curves for CH_3^+ and NH_3, respectively, obtained by the direct integration of the H-F force curves given in Figs. 3 and 5. By virtue of the floating, the curves of the integrated

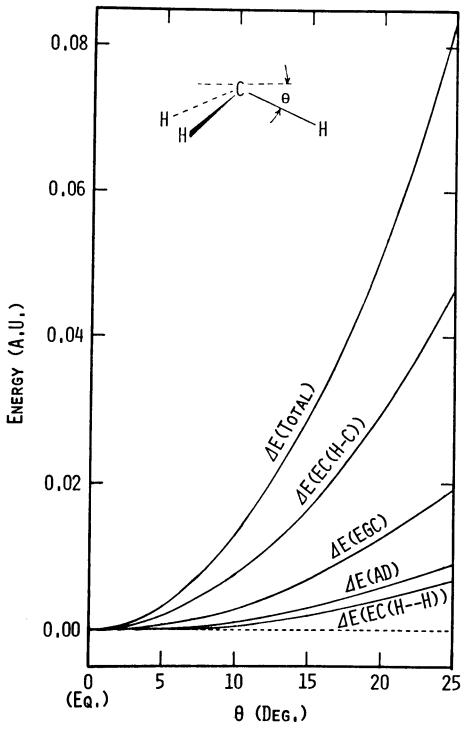

Fig. 6. Partitioning of the potential energy curve into the force theoretic terms for CH_3^+.

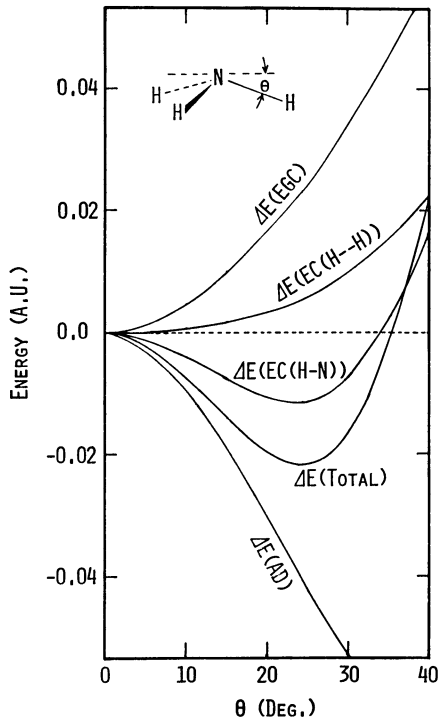

Fig. 7. Partitioning of the potential energy curve into the force theoretic terms for NH_3.

H-F forces (denoted as ΔE(Total)) are just superposable with the SCF energy curves shown in Figs. 3 and 5. The partitioning of the ΔE(Total) curve into the force theoretic terms given in Figs. 6 and 7 helps to analyze the potentical energy curve in terms of the regional roles of the electron-cloud reorganization during the bending process. The electron-cloud incomplete following in CH_3^+ shown in Fig. 2 works to destabilize the system as seen in the ΔE(EC(H–C)) and ΔE(AD) curves given in Fig. 6. It is the main origin of the potential energy curve ΔE(Total). For NH_3, the electron-cloud preceding in the atomic and overlap regions works to stabilize the molecule as seen from the ΔE(AD) and ΔE(EC(H–N)) curves in the angular region $0° < \theta < \theta_{eq}$. In the region $\theta > \theta_{eq}$, the electron-cloud incomplete following works to destabilize the system as seen in the ΔE(EC(H–N)) curve. For both CH_3^+ and NH_3, the parallelism between the ΔE(EC(H–A)) curve and the total curve is surprising. The same trend was also seen previously for H_2O.[19] Thus, it is confirmed that the density-guiding rule certainly shows the path along which the energy becomes lower most effectively.

Concluding Remarks

In this paper, we have studied the force and density origins of the molecular shapes of CH_3^+ and NH_3 on the basis of the floating wavefunctions which satisfy the H-F theorem for the force acting on the terminal protons. The present results may be summarized as follows:

1) The floating of the AO's gives a freedom in the wave function to describe an appropriate behavior of

the electron density especially in the atomic region. The direction and the extent of the floating of the FAO's accord with those expected from the general behaviors of the electron density, *i.e.*, the electron-cloud preceding and incomplete following. The effect of the floating on the H-F force is largest for the AD force.

2) For the floating wave function, the simple and pictorial concepts of the force theory holds in a sufficient accuracy. On this basis, we have confirmed that the previous concepts of the ESF theory correctly grasp the origins of the molecular shapes. The density-guiding rule based on the behaviors of the electron density is verified as the rule for the density origin. The force origin which is the AD and EC(H–A) forces reflects and quantifies the density origin. The roles of the other forces are also easily predicted by the ESF theory.

Lastly, it would be important to remark about an interpretation why the electron-cloud preceding or the incomplete following occurs in the A–H bond region under the bending process. Recently, Deb has given a postulate that the highest occupied molecular orbital (HOMO) would be most responsible for these behaviors since the HOMO is most weakly bound to the nuclear framework.[13] He has tried to systematize various molecular geometries on the basis of the "HOMO postulate."[12,13] Though this idea is interesting, this assumption seems to feel difficulty for larger molecules since they have many levels in the vicinity of the HOMO. The electron-cloud preceding and the incomplete following, which should be the density origin even for larger molecules,[9] are the behaviors of the *total* electron density. On the other hand, when we focus our attention on the force acting on the central atom (*e. g.* the atom A of the AH_3), we can easily predict the behaviors of the electron density on the basis of the chemically transferable concepts like lone pair, bond, gross charge, and the various effects on them (*e. g.* substituent effect), as has been shown previously in the ESF theory.[8] Therefore, we believe that for predictive applications, it is easier and more fruitful to focus our attention to the force acting on the central atom, except for the problems of the internal rotation barrier.[8] An *ab initio* verification of this approach will be given in the succeeding paper.

The authors would like to thank Dr. S. Yamabe, Dr. K. Kitaura, and Professor K. Morokuma for the use of the modified version of the Gaussian 70 Program, and Mr. S. Kanayama for the assistance of some computations. This study has been supported partially by the Scientific Research Grants from the Ministry of Education and by the Japan-U.S. Cooperative Science Program from the Japan Society for the Promotion of Science.

References

1) H. Hellmann, "Einführung in die Quantenchemie," Deuticke, Vienna (1937), p. 285; R. P. Feynman, *Phys. Rev.*, **56**, 340 (1939).

2) An exaustive review for the force concepts in chemistry has been given in a) B. M. Deb, *Rev. Mod. Phys.*, **45**, 22 (1973). and will appear in b) B. M. Deb, Ed., "The Force Concept in Chemistry," Macmillan, Bombay, in press. The Japanese readers may also refer to the following reviews written in Japanese; c) H. Nakatsuji, *Kagaku*, **28**, 17, 108 (1973); d) H. Nakatsuji, *Kagaku No Ryoiki*, **30**, 881 (1976).

3) T. Berlin, *J. Chem. Phys.*, **19**, 208 (1951).

4) R. F. W. Bader, W. H. Henneker, and P. Cade, *J. Chem. Phys.*, **46**, 3341 (1967), and the succeeding papers.

5) R. F. W. Bader and A. K. Chandra, *Can. J. Chem.*, **46**, 953 (1968).

6) J. O. Hirschfelder and M. A. Eliason, *J. Chem. Phys.*, **47**, 1164 (1967).

7) R. F. W. Bader and A. D. Bandrauk, *J. Chem. Phys.*, **49**, 1666 (1968); R. F. W. Bader, I. Keaveny, and G. Runtz, *Can. J. Chem.*, **47**, 2308 (1969).

8) a) H. Nakatsuji, *J. Am. Chem. Soc.*, **95**, 345, 354, 2084 (1973); b) H. Nakatsuji and T. Koga, Chap. 4 of Ref. 2b.

9) a) H. Nakatsuji, *J. Am. Chem. Soc.*, **96**, 24 (1974); b) *ibid.*, **96**, 30 (1974).

10) a) H. Nakatsuji, T. Kuwata, and A. Yoshida, *J. Am. Chem. Soc.*, **95**, 6894 (1973); b) H. Nakatsuji, T. Koga, K. Kondo, and T. Yonezawa, *J. Am. Chem. Soc.*, **100**, 1029 (1978).

11) H. Nakatsuji and T. Koga, *J. Am. Chem. Soc.*, **96**, 6000 (1974); T. Koga and H. Nakatsuji, *Theoret. Chim. Acta*, **41**, 119 (1976).

12) B. M. Deb, *J. Am. Chem. Soc.*, **96**, 2030 (1974); B. M. Deb, P. N. Sen, and S. K. Bose, *ibid.*, **96**, 2044 (1974).

13) B. M. Deb, *J. Chem. Educ.*, **52**, 314 (1975); B. M. Deb, S. K. Bose, and P. N. Sen, *Indian J. Pure Appl. Phys.*, **14**, 444 (1976).

14) L. Salem and E. B. Wilson, Jr., *J. Chem. Phys.*, **36**, 3421 (1962); L. Salem and M. Alexander, *ibid.*, **39**, 2994 (1963).

15) A. C. Hurley, *Proc. R. Soc. London, Ser. A*, **226**, 170, 179, 193 (1954); A **235**, 224 (1956); C. A. Coulson and A. C. Hurley, *J. Chem. Phys.*, **37**, 448 (1962).

16) A. C. Hurley, "Molecular Orbitals in Chemistry, Physics, and Biology," ed by P.-O. Löwdin and B. Pullman, Academic, New York (1964), p. 161.

17) G. G. Hall, *Phil. Mag.*, **6**, 249 (1961).

18) J. O. Hirschfelder, W. Byers Brown, and S. T. Epstein, *Adv. Quantum Chem.*, **1**, 255 (1964).

19) H. Nakatsuji, K. Matsuda, and Yonezawa, *Chem. Phys. Lett.*, **54**, 347 (1978).

20) P. Hohenberg and W. Kohn, *Phys. Rev.*, **136**, B864 (1964).

21) E. B. Wilson, Jr., *J. Chem. Phys.*, **36**, 2232 (1962); see also A. A. Frost, *ibid.*, **37**, 1147 (1962); S. T. Epstein, A. C. Hurley, R. E. Wyatt, and R. G. Parr, *ibid.*, **47**, 1275 (1967); H. Nakatsuji and R. G. Parr, *ibid.*, **63**, 1112 (1975).

22) The STO-3G expansion coefficients and exponents used here are those included in the Gaussian 70 Program.

23) W. J. Hehre, R. F. Stewart, and J. A. Pople, *J. Chem. Phys.*, **51**, 2657 (1969).

24) W. A. Lathan, L. A. Curtiss, W. J. Hehre, J. B. Lisle, and J. A. Pople, *Prog. Phys. Org. Chem.*, **11**, 175 (1974).

25) The explicit formulas for the AD, EC, and EGC forces used in the present calculations are the same as those given in Ref. 8b, except that the net-exchange force integral is modified as

$$\langle \chi_{rA} | (\boldsymbol{f}_A)_0 | \chi_{sB} \rangle \equiv \langle \chi_{rA} | \boldsymbol{f}_A | \chi_{sB} \rangle - \frac{1}{2} S_{rAsB} \times \{ \langle \chi_{rA} | \boldsymbol{f}_A | \chi_{rA} \rangle + \langle \chi_{sB} | \boldsymbol{f}_A | \chi_{sB} \rangle \},$$

where the first term in the brace was added here. It vanishes for the non-floating wave function.

26) H. Shull and D. Ebbing, *J. Chem. Phys.*, **28**, 866 (1958).
27) B. Roos and P. Siegbahn, *Theoret. Chim. Acta*, **17**, 199 (1970).
28) R. Moccia, *Theoret. Chim. Acta*, **8**, 8 (1967); P. Pulay, *Mol. Phys.*, **17**, 197 (1969).
29) S. D. Peyerimhoff, R. J. Buenker, and L. C. Allen, *J. Chem. Phys.*, **45**, 734 (1966); R. E. Kari and I. G. Csizmadia, *ibid.*, **50**, 1443 (1969); G. V. Bünau, G. Diercksen, and H. Preuss, *Int. J. Quantum Chem.*, **1**, 645 (1967).
30) Though the electron-cloud preceding and incomplete following are the behaviors of the *total* electron density, they are more visually depicted when an appropriate reference density is introduced. Since we are concerned here only in the electron density in the A–H region, we have introduced as the reference density the one obtained at $\theta=0°$ since it is symmetric with respect to the A–H axis. Therefore, the present difference density maps show chiefly the electron-cloud reorganization induced by the out-of-plane bending displacements.
31) At $\theta=40°$ we have used as the difference density the density obtained at $\theta=24.3°$ (calculated equilibrium), since there the transverse force is zero and the N–H bond density is almost symmetric with respect to the N–H axis. These two features are common to the planar form used as the reference at $\theta=15$ and 24.3°.
32) P.-O. Löwdin, *Phys. Rev.*, **97**, 1474 (1955).